JOURNAL OF THE PHYSICAL SOCIETY OF JAPAN Vol. 17, SUPPLEMENT A-III, 1962
INTERNATIONAL CONFERENCE ON COSMIC RAYS AND THE EARTH STORM Part III

III-4-20. Energy Spectrum of Nuclear Active Particles as Determined by a Total Absorption Spectrometer at 2.2 kms.

R. RAGHAVAN, B. V. SREEKANTAN, A. SUBRAMANIAN and S. D. VERMA

Tata Institute of Fundamental Research, Bombay, India

1. The energy spectrum of nuclear active particles in the energy range $2 \cdot 10^{11}$ ev to 10^{13} ev has been determined at mountain altitude of 2.2 kms (800 g/cm²) using a total absorption spectrometer.

The spectrometer (Fig. 1) has an effective area of 114 cm×122 cm and consists of alternate layers of iron and end-window liquid scintillation tanks stacked one above the other to a total height of about 2.5 meters. Each layer of iron is 4 cm thick (30 g/cm²).

The liquid scintillation tanks are of dimension 130 cm×60 cm×2.5 cm and are fabricated from alminum sheets. In each layer two tanks are placed one behind the other, with the glass windows facing two sets of photomultipliers which are DuMont 6364's and are mounted about a meter from the front surface of the spectrometer. The arrangement of photomultipliers is such that the first two sections serve to distinguish between the soft component and nuclear active particles. The amplifiers and two oscilloscope display system are designed to cover a range of 10^4 *i.e.* 10^9 ev to 10^{13} ev for the energy of nuclear active particles.

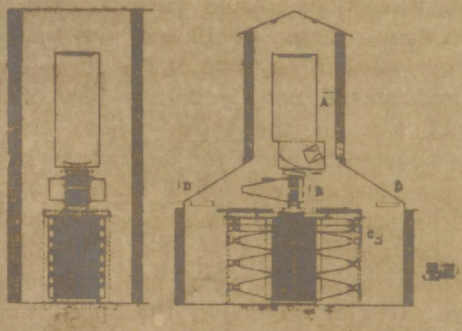

Fig. 1. Experimental arrangement at Ootacamund: Total Absorption Spectrometer, Cloud Chamber and Air Cerenkov Counter.
A=Air Cerenkov Counter.
B=Multiplate Cloud Chamber.
C=Total absorption Spectrometer.
D=Scintillation Counter Trays.

For triggering the spectrometer for nuclear active particles, the pulses from the 5 photomultipliers are added after suitable amplification, and passed through a discriminator, the bias of which could be set at any desired level. For determining the associated spectrum, four plastic scintillators two of area 0.36 m², and two of area 0.25 m² are placed around 1.70 m from the spectrometer. The amplitudes of pulses from these four scintillators are also recorded on an oscilloscope.

The spectrometer is shielded on all sides with 2″ of iron and 1″ of lead to minimize the energy flow from side showers.

2. Calibration of the spectrometer and errors in energy measurements.

The spectrometer was calibrated using a telescope to trigger the oscilloscope sweeps for vertical cosmic ray particles (μ-mesons) passing through the spectrometer. The average pulse heights thus obtained from the various photomultipliers were related to energy loss by ionisation of fast μ-mesons in the different sections. We have taken 48 Mev as the energy loss per layer of iron (30 g/cm²) and liquid scintillator.

In using the spectrometer to measure the energies of nuclear active particles, one has to consider the errors due to the following:

(a) errors in calibration and measurement of pulse heights
(b) sampling inefficiency due to the finite striations of the spectrometer
(c) leakage of energy due to finite thickness of the spectrometer.

The errors due to (a) are estimated to be not more than about 10% but those due to

* This paper was combined with III-4-19, III-4-21 and presented by B. V. Sreekantan.

(b) and (c) are somewhat uncertain.

The striation used here of 30 g/cm² of iron is fairly efficient in sampling energy transferred to π^0-mesons in the nuclear cascade; for example even at energies ~1 Bev, the electron photon track lengths are sampled to an accuracy of about 10%. The chief uncertainty comes from energy loss in nuclear disintegrations in iron and production of slow secondaries which are absorbed in a layer itself. It is difficult to estimate this mode of unsampled energy loss, since it involves details of propagation of the nuclear cascade in iron.

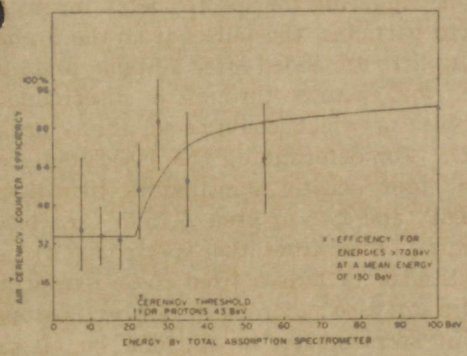

Fig. 2. Efficiency of Cerenkov counter for nuclear active particles as a function of energy observed in the total absorption spectrometer.

To get an idea of this energy loss, we have observed the efficiency of an air Cerenkov counter placed above the cloud chamber which in turn is kept above the spectrometer. Fig. 2 shows such an efficiency plot for nuclear active particles identified by interactions inside the chamber. The break in the efficiency curve indicates that at an energy of 43 Bev for a nuclear active particle incident on top of the spectrometer only 21 Bev is measured in it. This indicates the magnitude of this energy loss. It is to be expected that the fraction of the primary energy unsampled in this manner would decrease with increasing energy because of the increase of energy transferred to π^0-mesons compared to the almost constant energy loss through slow particles (this can be taken to be~1 Bev per collision in iron) in nuclear collisions. The exact variation of the unsampled energy loss is not amendable to calculation without invoking nuclear cascade models. As a first approximation, we have assumed that energies measured by the spectrometer if shifted by 20 Bev would give the correct total energy dissipated in the spectrometer for energies up to 100 Bev. For energies much above 100 Bev the correction can be expected to be a negligible fraction of the primary energy.

Regarding (c), it is not easy to estimate the magnitude of this loss exactly, but if inelasticity of nucleons in collisions with iron nuclei is not too small (*i.e.* inelasticity ≥ 0.5), one can expect~15% of the incident energy to leak out of the spectrometer (~6 m.f.p. for nuclear interactions). If the above mentioned inelasticity factor is not strongly energy dependent, one can expect this fractional leakage energy to be independent of the energy of the incident nuclear active particle.

3. Criteria for the selection of nuclear active particles traversing the spectrometer

A nuclear active particle above the set limit of trigger (100 Bev) is deemed to have passed through the spectrometer (right half or left half) and interacted whenever there were comparable sequence of pulses in at least the three lower sections of corresponding half of the spectrometer with or without energy flow in the top two sections. It is further demanded that in such a sequence of pulses, the energy losses that occurred in adjacent sections should have a ratio not more than a factor of 10 and also that the energy losses in any two of the three lower sections should not be both ~10% of the energy loss in the third. These criteria were adopted to allow for fluctuations in the cascade development of a nuclear active particle accepted to have passed through the spectrometer and at the same time to discriminate against very inclined nuclear active particles traversing the spectrometer suffering only partial energy loss in the spectrometer. It is thought that no energy dependent bias is introduced by the above procedure since the cascade of nuclear active particles, judged from events observed in the cloud chamber for energies greater than 100 Bev (the trigger limits for obtaining the spectra have been set above this value), have ranges of the order of the entire depth

of the spectrometer and definitely satisfy the above ratio requirements in energy losses in the different sections. With these criteria it was possible to distinguish the incidence of one or more nuclear active particle in each half of the spectrometer from cases of inclined nuclear active particle traversing part of both halves of the spectrometer from a scrutiny of the pulse height distributions in the different sections of the two halves of the spectrometer.

A nuclear active particle is considered to have been accompanied by an air shower when more than one of the plastic scintillators kept near the spectrometer indicated passage of at least one minimum ionizing particle through them or there was energy flow due to electron-photon component in both halves of the spectrometer on top when only one plastic scintillator registered particles. In cases where a nuclear active particle is judged to be accompanied by air showers, the energy in the top two sections of the spectrometer were not added to the energy of the nuclear active particle; this was done only if the second section energy loss was less than or equal to the energy loss in the first section. In other cases, twice the energy registered by the first section was considered to be the energy flow due to soft component of air showers. This criterion is consistent with the expectation that even near cores of air showers the mean energy per electron is only~1 Bev.

Energy spectra

Data obtained during 101 hrs of operation of the spectrometer during which time trigger bias was set at 100 Bev for 27 hrs, and for the rest of the time at 250 Bev, were analysed. Fig. 3 gives the integral spectrum of nuclear active particles above 150 Bev for all nuclear active particles "associated" with air showers. The points at 150 Bev are considered to have a bias due to threshold effect. The two integral spectra can be represented as power laws with negative exponents 1.45 ± 0.15 and 1.25 ± 0.15 respectively.

It should be remarked that the two spectra as drawn here are not directly comparable (for fraction of "association" to total) because the data have not been normalised to the same operating time. The observed percentage of "association" at energies >250 Bev, is $81\pm9\%$. It is likely that this "association" has been enhanced by the high walls surrounding the spectrometer and some of the "associated" cases may be the result of true unassociated nuclear active particles in air just outside above the apparatus. It is also to be remarked that while the energy spectrum of all nuclear active particles is meaningful, it is difficult to interpret spectra termed "associated" and "unassociated" since the data is relevant only to the apparatus used. We give in Fig. 4, the integral spectrum of nuclear active particles obtained in the energy region

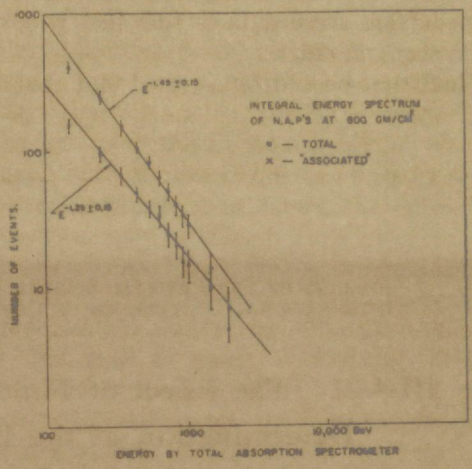

Fig. 3. Energy spectra of nuclear active particles obtained with the total absorption spectrometer (10^{11}–10^{12} ev).

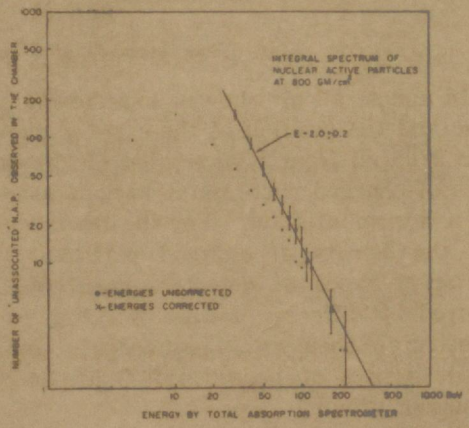

Fig. 4. Energy spectrum of "unassociated" nuclear active particles with the total absorption spectrometer (10^{10}–10^{11} ev), and cloud chamber.

10–100 Bev for events observed in the cloud chamber triggered for nuclear active particles "unassociated." The spectrum has a slope of 2.0 ± 0.2.

The absolute flux value for nuclear active particles at 800 gm/cm^2 for energies greater than 450 Bev deduced from our data is $(1\text{-}2.3) \pm 0.1 \times 10^{-7}$ particles cm^{-2} sec^{-1} sterad^{-1}. The uncertainty in the flux comes from the inexact definition of solid angle of acceptance for the spectrometer by the selection criteria detailed above. This value is consistent with the value expected from other similar estimates made at mountain altitudes reduced to our altitude by using an absorption mean free path for the nuclear active particles value of 120 g/cm^2. The flux expected from these data is 1.6×10^{-7} particles cm^{-2} sec^{-1} sterad^{-1}.

Finally, it should be pointed out that the measured energy spectrum of nuclear active particles would deviate from the true spectrum at sufficiently high energies depending upon the size of the detectors used. This is because at high energies depending upon the size of detectors used, many nuclear active particles are incident at the same time over the area of a single detector, the effect of which will be to flatten the spectrum. It will be ambiguous to interpret spectra obtained without considering this effect. For example, the average separation of nuclear active particles at 10^{12} ev for simultaneously incident particles are expected to be of the order of 70 cm and hence spectra deduced with detectors ~ 1 m^2 (as is our case) for energies $> 10^{12}$ ev lose their significance unless other means of resolution of nuclear active particles are incorporated in such large detectors.

JOURNAL OF THE PHYSICAL SOCIETY OF JAPAN Vol. 17, SUPPLEMENT A-III, 1962
INTERNATIONAL CONFERENCE ON COSMIC RAYS AND THE EARTH STORM Part III

III-6-4. Characteristics of High Energy Nuclear Interactions*

An Experimental Study with the Combined Techniques of Multiplate Cloud Chamber, Air Cerenkov Counter and Total Absorption Spectrometer

Siddheswar LAL, R. RAGHAVAN, B. V. SREEKANTAN,
A. SUBRAHRANIAN and S. D. VERMA

Tata Institute of Fundamental Research,
Bombay, India

An experiment is in progress at Ootacamund (2.2 km altitude corresponding to 800 gm/cm² pressure) to study the characteristics of high energy nuclear interactions induced by cosmic ray particles of energies ≥ 30 Bev. The plan of the experimental arrangement is shown in Fig. 1. A multiplate cloud chamber of dimensions $60 \times 60 \times 20$ cm³ having two producing layers of graphite each 4 cm in thickness is placed above a total absorption spectrometer described in detail in another paper in this proceedings (III-4-20). The total absorption spectrometer gives a measure of the energy of an incident particle producing a nuclear interaction in the carbon inside the chamber. The chamber has five 1/4″ brass, one 3/4″ brass and two 1/2″ lead plates below the graphite blocks in that order to measure the energies of γ-rays produced by the decay of neutral pions originating in the nuclear interaction in the graphite blocks. A spacing of about 10 cm is given between the producer and the first brass plate, so that the secondaries from the interaction in graphite to diverge and enable the measurement of the angular distribution at the point of production.

The chamber is triggered whenever Geiger counter trays just above and below the chamber have a coincident discharge simultaneous with the occurrance of two or more particles in a liquid scintillator below the chamber attended by energy release of at least 10 Bev in the spectrometer. Two Geiger counter trays of area 1/2 m² each kept near the chamber, feed pulses in anticoincidence with the above trigger pulse to eliminate air showers. In addition, an air Cerenkov counter is placed above the chamber which enables us to distinguish whether an incident particle producing a nuclear interaction in the chamber is a proton or a pion, if the energy of the incident particle is known to be less than 40 Bev. This is known only in part of the cases since additional detectors like Geiger tray on top of the air Cerenkov counter were required to be set off before information from the air Cerenkov detector was considered. For obtaining reliable information from the air Cerenkov detector, it was demanded that only one charged particle was incident on

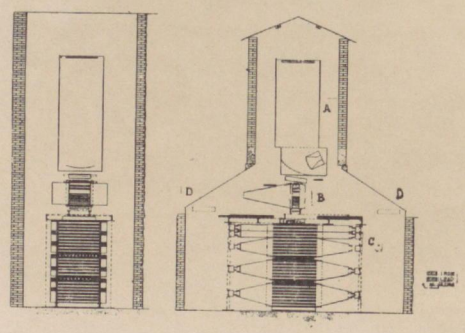

Fig. 1. Experimental arrangement at Ootacamund.

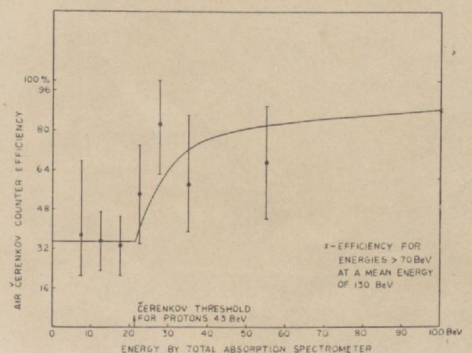

Fig. 2. Efficiency of Cerenkov counter for nuclear active particles as a function of energy observed in the total absorption spectrometer.

* This paper was read by M. G. K. Menon.

the effective area of the air Cerenkov counter. Results presented here are based on an analysis of 30 nuclear interactions observed in the graphite layers inside the cloud chamber. This represents only part of the data collected so far.

Corretion for the energy measurements by the total absorption spectrometer was determined by studying the variation of efficiency of the air Cerenkov counter with the energy of the nuclear active particles, (which were identified by their interactions in the cloud chamber and whose energies were determined by the total absorption spectrometer). This variation is shown in Fig. 2. A break in the efficiency at 21 Bev is identified as the Cerenkov threshold energy of 43 Bev for protons. The fall in efficiency below this threshould shows that $40\pm9\%$ of the charged nuclear active particles are pions near an energy of 30 Bev. The above effiiciency plot indicates that at a proton energy of 43 Bev, about 22 Bev is dissipated in energy losses in the spectrometer (heavy fragments) which is not sampled by the liquid scintillators. The observed energy loss distribution in the spectrometer for nuclear active particles of these energies, shows that very little energy escapes from the spectrometer (750 gm/cm^2 of Fe in total). As a first approximation, the spectrometer energies were shifted by 20 Bev as a systematic correction for invisible losses

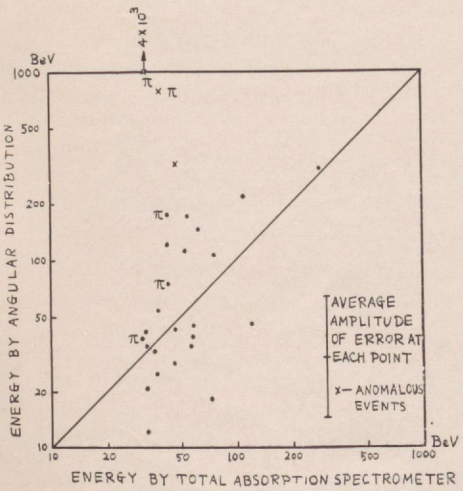

Fig. 3. Plot of primary energy estimated from the angular distribution of the secondaries by the method employed by Castagnoli *et al.* against the energy measured by total absorption spectrometer suitably corrected for unsampled energy losses.

at the energies involved here. The actual energy measured from the spectrometer is accurate to within 10% but the correction for invisible energy lossses are uncertain and could be an underestimate at energies >40 Bev.

Fig. 3 shows a plot of energies of 27 nuclear active particles observed to produce nuclear interactions ($n_s \geq 3$) in the graphite blocks inside the chamber. The sum of the energy observed in the spectrometer and the visible energy in the cloud chamber is plotted on the abscissa and the energy deduced from the angular distribution of the secondaries of the interaction by the well known formula:

$$\log \gamma_c = \frac{1}{n_s} \Sigma \log \cot \theta_i$$

on the ordinate. The amplitude of error at each point for the angular distribution method was taken to be given by

$$\Delta \log \gamma_c = \frac{0.36}{\sqrt{n_s}}$$

which is indicated in the figure for $n_s=5$. Except for the three cases indicated by crosses, the energy estimates by the two methods may be considered to be in agreement. The points marked by crosses show considerable deviation (more than two standard deviations). It is interesting to note that two of these anomalous cases are likely to be pions as deduced from the response of the air Cerenkov counter. It is also interesting to note that in general pion interactions seem to have energy estimated by the angular distribution method higher than that given by the spectromenter. It is conceivable that such an overestimate of the primary energies in the case of pion interactions could be due to the target mass participating in such collisions being smaller than that of a nucleon, probably of the order of pion mass itself. As regards the "normal" events the nature of whose primaries are not indentified, considering the fact that about 40% of them would be due to pions as estimated earlier, we can say that in a majority of nucleon-nucleon collisions at energies ~50 Bev, there are no sharp asymmetries of angular distribution of secondaries in their center of mass. (Figs. 4, 5 and 6 are examples of some of the events obtained.)

The average fast charged secondary mul-

tiplicity (n_s) for the cases of identified pion interactions is 4 ± 1. This value applies to the energy region 30–40 Bev. For the cases of other charged primary interactions in the energy region 30–60 Bev, the mean charged multiplicfty is 5.7 ± 0.6 after correcting for forward protons. γ-ray energies have been estimated from the track lengths and shower development in the plates. For eighteen events in the primary energy range 30–60 BeV, the fractional energy radiated as pions is $3\Sigma E_{\pi 0}/E_0=13$–17%. The upper limit in the above value results from indistinguishability of γ-rays from secondary interactions in a few cases and also from estimates of energies of γ-ray showers which are only partially absorbed in the plates in certain cases. A correction has to be applied for loss of γ-ray at large angles to the direction of incident primaries. A rough upper estimate of this can had, if we assume that π°-mesons emitted in the backward direction in the centre of mass system of the collision would give rise to γ-rays which would be lost for observation in the chamber. This leads to an increase of K_π deduced above by 30% if we assume that π°-mesons are emitted isotropically with a mean energy independent of the primary energy. The statistical error of the estimate of K_π is about 25%.

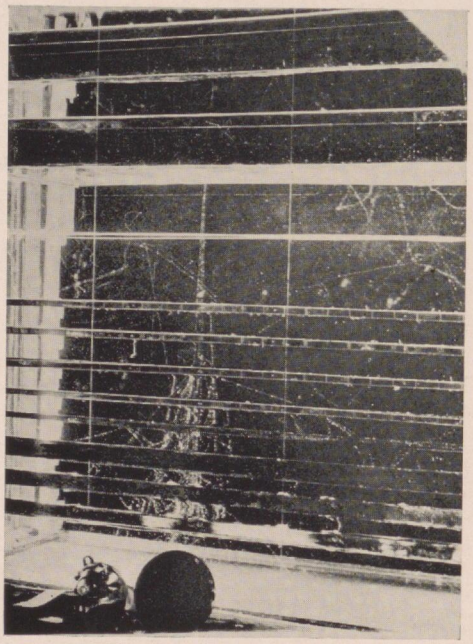

Fig. 4. An example of an interaction induced most probably by a pion which gives rise to an anomalous case plotted in Fig. 3. An energy estimate of $800\ {}^{+1200}_{-\ 500}$ Bev is given by the angular distribution method, which the spectrometer gives an energy less than 40 Bev.

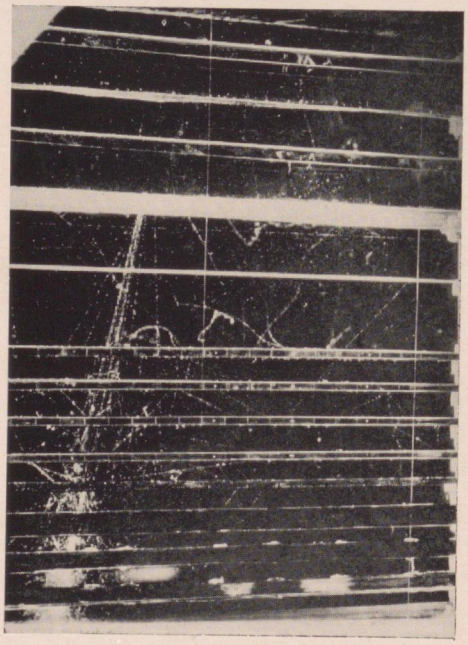

Fig. 5. A case of agreement between the two methods. Estimate by angular distribution method gives $316\ {}^{+234}_{-134}$ Bev and that by total absorption spectrometer is 258 Bev.

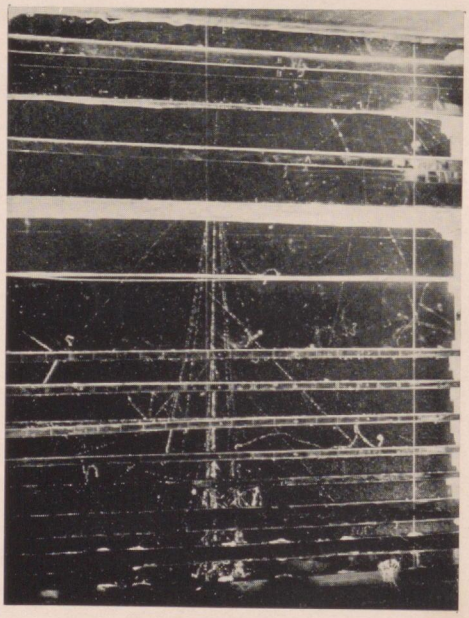

Fig. 6. A case where total absorption energy is in excess of the energy from angular distribution but the deviation is less than two standard deviations. The former gives 124 Bev and the latter $50\ {}^{+44}_{-23}$ Bev.

JOURNAL OF THE PHYSICAL SOCIETY OF JAPAN Vol. 17, SUPPLEMENT A-III, 1962
INTERNATIONAL CONFERENCE ON COSMIC RAYS AND THE EARTH STORM Part III

III-4-25. Study of Core Structure of Small Size Air Shower

S. MIYAKE, B. V. SREEKANTAN, P. V. RAMANAMURTHY,
V. S. NARASIMHAN, S. D. VERMA, G. T. MURTHY
and B. K. CHATTERJEE

Tata Institute of Fundamental Research, Bombay, India

The density spectrum and the energy spectrum have been observed at sea level and at mountain altitude (800 g cm^{-2}) with AS tray. The exponent of density spectrum was obtained as -1.53 ± 0.1 at 800 g cm^{-2} and -1.55 ± 0.1 at sea level. The exponent of total energy flow spectrum was obtained as -1.7 ± 0.1 at both altitudes. The exponents of the energy flow spectra with AS coincidence both at sea level and at mountain altitude are found to continuously steepen with increasing energy flow. And the spectrum varies largely depending on the condition of AS coincidence. From these features, we found that (1) there is a clear change in the character of core at about 10^5 in size of EAS and (2) the change comes from interaction character in high energy region. The series of observation is continuing by means of water spectrometer and preliminary results are presented.

In the past several experiments were done on the density spectrum of extensive air showers—a review of most of this earlier work by Greisen[1] can be found in progress in cosmic ray physics Vol. III. Since this review, there was another experiment reported by Green and Barcus[2]. In all these experiments, the frequency of occurrence of air showers with various densities over the apparatus was studied without any reference to the energy content of the electrons producing these densities. We have done an experiment both at sea level and at mountain altitude (800 g cm^{-2}) wherein we measured the density spectrum of EAS in this usual way and, in addition, the energy flow spectrum of EAS.

The experimental set up is shown in Fig. 1. Two plastic scintillators (designated T and B) were kept one above the other with a layer of lead having a thickness of 2.5 cm in between them. Besides these two, there was a third plastic scintillator (designated AS) at distance of 2 m.

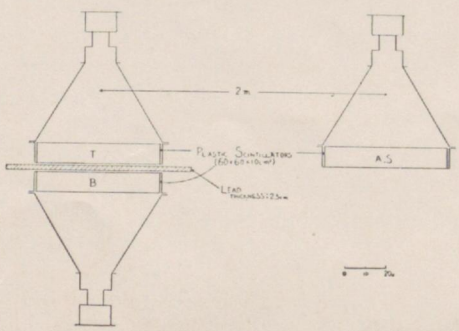

Fig. 1.

The results on the density spectrum (T+AS) and on the energy flow spectrum (B+AS) of EAS both at sea level and at mountain altitudes are presented in Fig. 2. The frequencies of occurrence of pulses of various sizes in the top and in the bottom scintillators without any demand on the air shower scintillator are also shown in the same figure (curves designated as T and B). The exponent of the density spectrum in the region of densities 15/m^2 to 800/m^2 as obtained by us is -1.53 ± 0.1 at 800 g/cm^2 and -1.55 ± 0.1 at sea level. The two exponents of the density spectrum at mountain altitude and at sea level are the same within experiment errors. There is no disagreement with the earlier work on this. The exponent of total energy flow spectrum was obtained as -1.7, and the exponents of the energy flow spectra with AS coincidence both at sea level and at mountain altitudes are found to continuously steepen with increasing energy flow. There seems to be no significant difference in the exponent of the energy flow spectra at mountain altitude and at sea level. It may be pointed out by us as was done several times before by

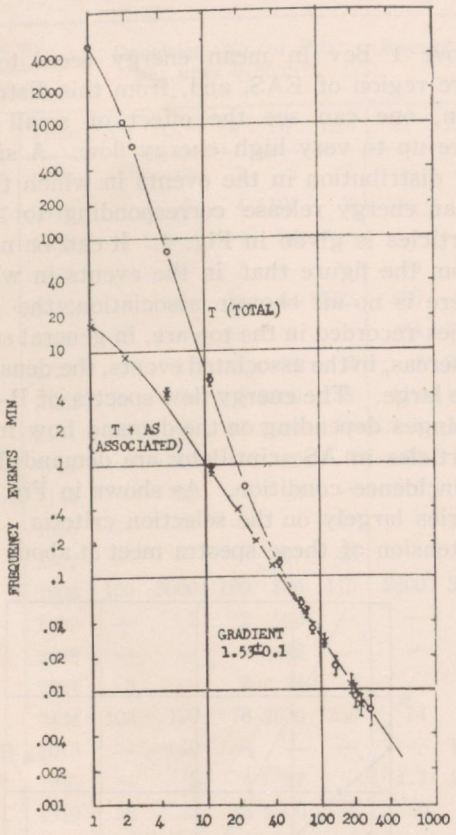

Fig. 2a. 800 gcm^{-2} T and T+AS.

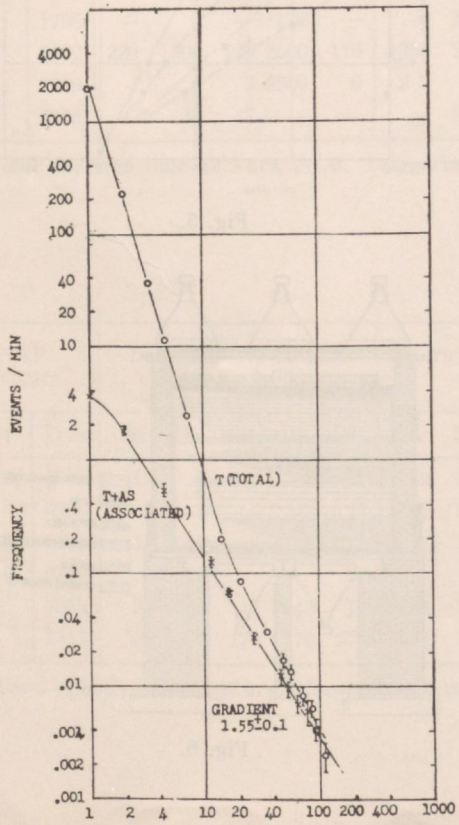

Fig. 2b. Sea Level T and T+AS.

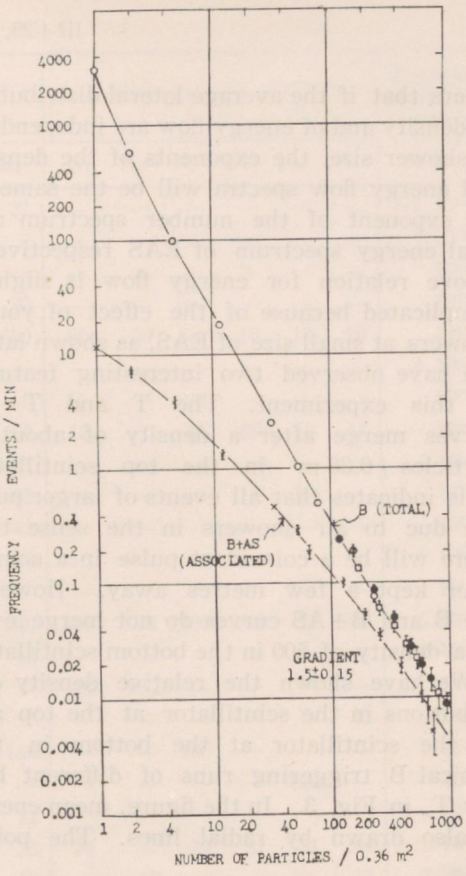

Fig. 2c. 800 gcm^{-2} B and B+AS.

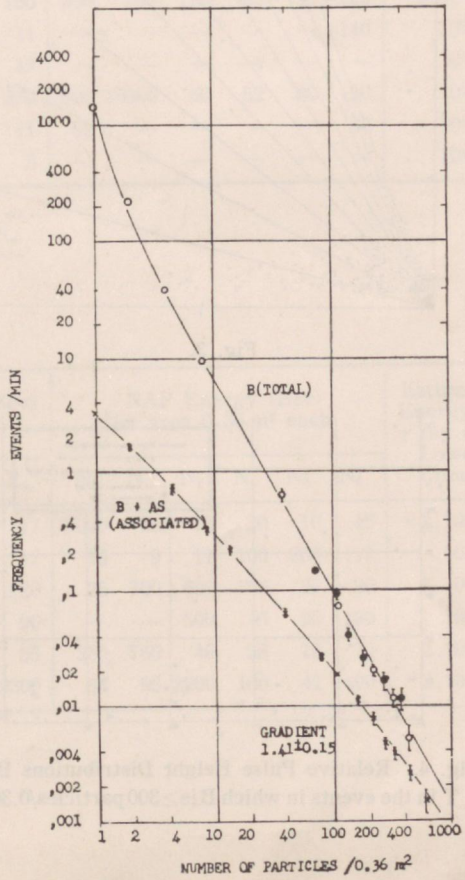

Fig. 2d. Sea Level B and B+AS.

others that if the average lateral distribution of density and of energy flow are independent of shower size, the exponents of the density and energy flow spectra will be the same as the exponent of the number spectrum and total energy spectrum of EAS respectively. Above relation for energy flow is slightly complicated because of the effect of young showers at small size of EAS, as shown later. We have observed two interesting features in this experiment. The T and T+AS curves merge after a density of about 50 particles / 0.36 m² in the top scintillator. This indicates that all events of larger pulse are due to air showers in the sense that there will be a coincident pulse in a scintillator kept a few metres away. However the B and B+AS curves do not merge even at a density of 500 in the bottom scintillator.

We have shown the relative density distributions in the scintillator at the top and in the scintillator at the bottom in two typical B triggering runs of different bias for T, in Fig. 3. In the figure, mean energy is also drawn by radial lines. The points above 1 Bev in mean energy seem to be core region of EAS, and, from this distribution, one can see the effect of small size core up to very high energy flow. A simillar distribution in the events in which there is an energy release corresponding to ≥300 particles is given in Fig. 4. It can be noted from the figure that in the events in which there is no air shower association, the densities recorded in the top are, in general small whereas, in the associated events, the densities are large. The energy flow spectra of B+AS changes depending on the demand how many particles in AS scintillator are demanded for coincidence condition. As shown in Fig. 5 it varies largely on the selection criteria. The extension of these spectra meet at about 1000

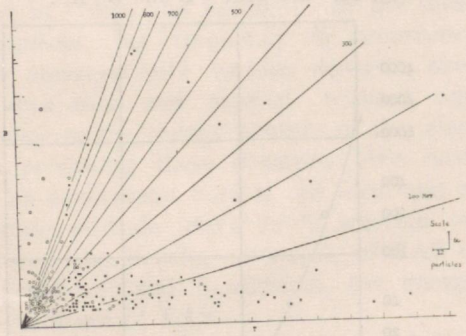

Fig. 3.

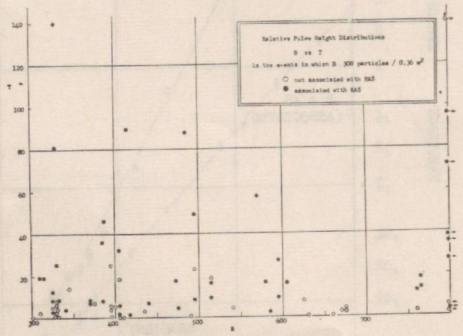

Fig. 4. Relative Pulse Helght Distributions B vs T in the events in which B is ≥300 particles/0.36m²

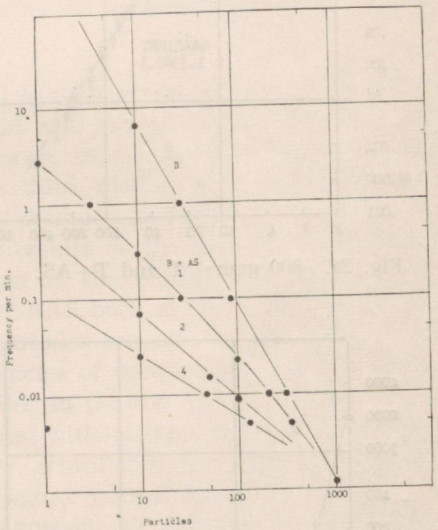

Fig. 5.

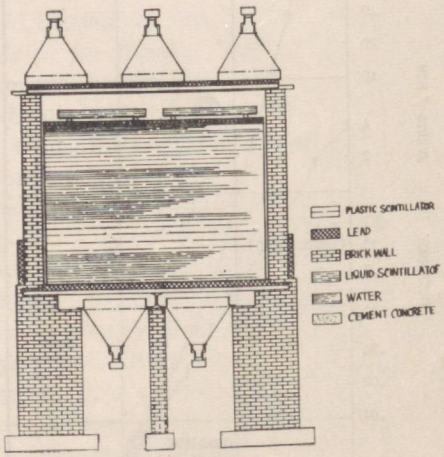

Fig. 6.

Table Ia.

Energy Flow Trigger		Densities (No. of Ptls per area 0.36 m²)					Energy Flow (Bev) 1 m²				NAP Energy (Bev)						Estimated Energy of γ-ray (ev) Lower Limit
Date	Time	D_1	D_2	D_3	D_4	D_5	E_1	E_2	E_3	E_4	N_1	N_2	N_3	N_4	N_5	N_6	
4-8-61	0919	—	80	3	4	2	—	—	13	27	—	—	—	—	—	—	$>4.10^{12}$
	0942	—	5	4	101	2	—	7	100	5	—	—	—	—	—	—	4.10^{12}
	1039	—	—	—	34	—	—	—	74	—	—	—	—	—	—	—	10^{12}
	1238	—	46	7	—	4	4	15	70	30	—	—	—	—	—	—	10^{12}
	1346	35	120	28	64	2550	350	26	21	600	60	26	—	10	10	20	10^{14}
	1524	37	—	10	—	—	84	110	2	—	—	—	—	—	—	—	4.10^{12}
	1725	—	1	1	38	2	4	280	260	—	—	—	—	—	—	—	10^{12}
	2122	56	78	58	2500	58	110	110	420	50	12	9	34	69	16	17	10^{14}
	2154	10	19	17	2500	12	8.5	110	150	11	—	—	—	—	—	—	10^{14}
5-8-61	0714	—	47	—	2	5	25	22	211	55	—	—	—	—	17	—	10^{12}
	1114	—	38	—	2	—	5.6	11	90	42	—	—	—	—	—	—	10^{12}
	1550	—	78	—	—	—		1.5	210	10	—	—	—	—	—	—	4.10^{12}
	1802	—	—	—	37	40			140		—	—	—	—	—	—	10^{12}
	1902	100	5000	100	160	115	2600	300	7000	340	400	75	1700	100	35	180	5.10^{14}
	1927	—	2	2	520	—	—	—	7.4	42	—	—	—	—	—	—	2.10^{13}
	2048	—	—	—	52	—	—	—	390	—	19	180	—	—	—	—	10^{12}
	2201	3	—	2	34	—		45	45	7	—	—	—	—	—	45	10^{12}
	2424	122	190	78	2500	250	74	70	80	150	—	—	100	—	—	—	10^{14}
6-8-61	1013	—	40	—	—	—	—	140	—	—	—	—	—	—	120	—	10^{12}
	1055	—	3	4	47	—	1.7	2.5	300	12							10^{12}
	1319	36	82	48	2500	63	50	47	1700	35	75	—	11	21	11	84	10^{14}
	1407	3	2	5	390	5		8.2	100	10	—	17	—	—	—	12	2.10^{13}
	1449	43	90	4000	640	390	130	300	420	150	250	100	180	45	80	220	2.10^{14}
	1729	36	45	37	1900	40	8.5	25	100	11	—	—	—	—	—	140	10^{14}
	1736	—	6	—	170	—	—	1.1	70	17	—	—	—	—	—	—	10^{13}
	1952	220	300	125	2500	110	1350	300	1500	370	600	15000	60	52	80	20	10^{14}
	1959	4	6	5	2500	6	2.7	13	100	11	22	—	—	—	—	32	10^{14}
	2156	—	42	7	—	—	—	6.5	260	3	—	—	—	—	—	—	10^{12}

Total effective time 52.5 hrs. E. F. Triggering.

Table Ib.

NAP Trigger		Densities (No of Ptls per area 0.36 m²)					Energy Flow (Bev) 1 m²				NAP Energy (Bev) Det area 0.36 m² each						Estimated Energy of γ-ray (ev) Lower Limer
Date	Time	D_1	D_2	D_3	D_4	D^5	E_1	E_2	E_3	E_4	N_1	N_2	N_3	N_4	N_5	N_6	
7-8-61	0645	15	6	600	7	11	24	300	14	17	5000	26	11	30	10	15	2.10^{13}
	0956	3	2	—	7	37	1.5	3.6	5	17	13	9	11	100	900	17	10^{12}
8-8-61	0322	14	200	8	7	9	30	300	110	120	26	700	600	155	35	80	5.10^{12}
9-8-61	0739	3	6			37	—	—	—	90	—	—	500	13	22	160	10^{12}
	1529	23	350	17	43	17	3600	300	320	55	330	760	46	38	15	32	2.10^{13}
	1712	320	5000	170	170	370	3600	300	1200	9300	54	95	2200	100	42	1400	2.10^{14}

Total effective time=42 hrs. *N* component triggering.

particles in the bottom scintillator. Because of high mean energy, the events near the meeting point correspond to the core of various sizes. The result shows that the character of the core of EAS fluctuate largely below certain size which can be estimated from corresponding density or absolute frequency. In the series of this experiment, the critical size was estimated as about 10^5. From the observed frequencies of air showers (T+AS and B+AS) at sea level and at mountain altitude, the absorption length of rate was 115 ± 10 g/cm^2, then, we can conclude that the change of character in the core of EAS is not due to the primaries but to the character of interaction in high energy region.

Fig. 6 shows new arrangement to study the core structure of small size EAS. We can observe simultaneously density and core position at the top, and energy flow carried by soft component and of N-component which interact in the water tank. In the initial stage of construction, the water was not wed and six energy flow detectors were used to measure the area of highest energy flow which correspond to core region, and this was estimated as about 0.5 m in diameter. Later the water tank was set up and we found that the events triggered by energy flow are not mainly due to nucleon component since the rate did not change much with and without water. We are now taking runs with various kind of triggering namely, by the density, energy flow and nucleon component. The observation is now going on and some preriminaly result from the energy flow and nucleon component triggering runs are given in the following table for nearly same time of operation (52 and 42 hours respectively). The energy flow triggering is very useful to detect cores of small size EAS, and we find frequently the existence of steep cores which are probably due to γ-rays of energy greater than 10^{12} ev, as can be seen in the table.

References

1) K. Greisen: Progress in Cosmic Ray Physics Vol. III. (North Holland Publishing Compony, 1956).
2) J. R. Green and J. R. Barcus: Nuovo Cimento, **14** (1959) 1356.

JOURNAL OF THE PHYSICAL SOCIETY OF JAPAN Vol. 17, SUPPLEMENT A-III, 1962
INTERNATIONAL CONFERENCE ON COSMIC RAYS AND THE EARTH STORM Part III

III-4-21. The Effect of Finite Thickness of Scintillators on the Determination of the Densities of Charged Particles in Air Shower Experiments

B. K. CHATTERJEE, G. T. MURTHY, S. NARANAN,
T. N. RANGA SWAMY, B. V. SREEKANTAN
and M. V. SRINIVASA RAO

Tata Institute of Fundamental Research, Bombay, India

In almost all air shower experiments, the size and the position of the cores of showers are deduced from a knowledge of the densities of charged particles at various locations in a horizontal plane. For the determination of the density of charged particles, three different types of detectors are being employed by different groups working on extensive air showers. They are

(i) Arrays of hodoscoped G. M. Counters (Russian groups)

(ii) Arrays of Conversi type Neon tubes (I.N.S. Tokyo)

(iii) Scintillators (M.I.T., Cornell, I.N.S., Bombay, Sydney)

It is to be expected that the densities determined from G. M. counter arrays will be close to the true values of the densities of charged particles, since the G. M. counters are known to have very low efficiency for the detection of γ-rays and the amount of matter by way of wall thickness will be almost negligible for either absorption of electrons or for the interactions of nuclear active particles. If the efficiency of Neon Hodoscopes are also small for γ-rays, then

* This paper was combined with III-4-19, III-4-20 and presented by B. V. Sreekantan.

they should be as good as G. M. counters. It is quite definite that if one uses scintillators, for the determination of the densities, then a correction is necessary to obtain the true values of the densities. There are conflicting results regarding this correction factor. The M.I.T. group[1] from an analysis of showers in which densities were recorded both by scintillators (6 cm thick plastic) and G. M. counters find that the density values deduced from G. M. counters are comparable the density values deduced from scintillators. However this result is based on analysis of only 27 showers. On the other hand Wallace[2] finds that the density values deduced from scintillators (liquid 10 cm) are systematically higher than those deduced from G. M. counter—on the average the scintillators giving a density higher by about 34%. Wallace also finds that the ratio of densities depends on the shower size and cores distance. The increase in density in scintillators has been interpreted as due to nuclear interactions, in the scintillators. The I.N.S. group[3] find that the densities determined from Neon Hodoscopes differ from those of scintillators (plastic, thickness 4.5 cm) by a factor which depends on the distance from the core of the shower. In view of these conflicting results and since we have used scintillators in our air shower array (previous paper), we thought it worthwhile to investigate the dependence of the density values on the thickness of scintillators used. For this purpose, a variable level liquid scintillator was used in conjunction with the air shower array at Ootacamund. This liquid scintillator was placed just a meter away from one of the plastic scintillators. The level of the liquid was varied from 1 to 8 cm and about 1000 air showers were recorded for each thickness, after calibrating the scintillators for single particles. The density values as determined from the liquid scintillator were compared with the density determined by the neighbouring plastic scintillator. Preliminary results are shown in Fig. 1.

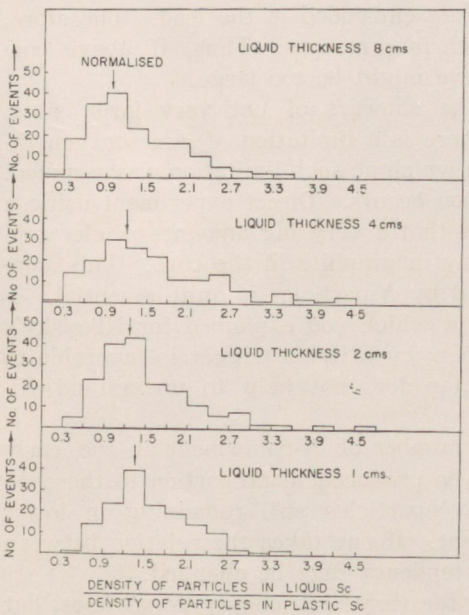

Fig. 1.

It is seen from Fig. 1, that with increasing thickness of liquid the density values decrease showing a slight absorption. The absorption mean free path is about 17–20 g/cm². The results indicate therefore that absorption of soft particles dominates over sensitivity to γ-rays and nuclear interaction at least up to a thickness of 8 cm of liquid. Further analysis of data is under progress and will be reported elsewhere.

References

1) G. W. Clark, J. Earl, W. L. Kraushaar, B. Rossi, F. Schreb and D. W. Scott: Phy. Rev. **122** (1961) 637.
2) Wallace: Proc. Moscow Conf. II (1959) 316.
3) S. Fukui, H. Hasegawa, T. Matano, I. Miura, M. Oda, K. Suga, G. Tanahashi and Y. Tanaka (Pre-print)

Discussion

Kasha, H.: I would like to ask at what distance from the core was the scintillator response measured?

I would like also to note that it has been also observed by the Imperial College shower group that the absorption of particles (in water) is more pronounced than their multiplication.

Sreekantan, B. V.: For the present analysis, we have considered showers striking at a distance of more than about 5 meters. We will be making a detailed analysis as a function of shower size and core distance.

Oda, M.: 1) Are fluctuation of N-particles and μ-mesons uniquely related?

2) In connection with the parallelism of fluctuations of μ-and N-component, is there any possibility that some part of μ-mesons observed were N-component?

Sreekantan: 1) We find that there is positive correlation in the fluctuations of μ-mesons and N-particles in all the cases we picked up as having fluctuations in the μ-component.

2) That is a remote possibility. However, I must point out that the separation between the three μ-detectors were of the order of 15 metres. All the three units showed fluctuations by the same extent as can be seen from table III. Also the amount of matter above the μ-mesons detectors was more than 5 interaction mean free paths. It is more likely that they are μ-mesons and not nuclear active particles.

Millar, D. D.: In view of the interesting result that there is a positive correlation between the fluctuations in nucleon and μ-meson numbers in showers of a given electron size, it might now be valuable to think rather of the fluctuations in the electron component in showers of a given nucleon or μ-meson size, such fluctuations arising from the interactions which have occured within the last two or three mean free paths above the apparatus rather than in the first collision. A relatively local origin for much of the electron component in an air shower may follow from the indication of nuclear emulsion work of a cut-off in the π° spectrum from jets.

Zatsepin, G. T.: It is very interesting to see the positive correlation between the fluctuations of μ-mesons and N-particles. I remember that Nikolsky's result showed a knee on the dependence of N-particles on the size. There, he selected the lowest size showers in the apparatus in which counters were embedded in the lead. Therefore, he might have selected showers which were rich in μ-mesons. Thus, if above correlation exists, the lowest size point on his curve might be too large.

Secondly, I would like to mention that for the showers of not very large sizes, there will be such fluctuation, provided that there is a limitation of π-meson generation. However, we have made a calculation in which no such limitation was assumed. Then, we still found that such a big fluctuation occurs. Direct experiment using a thick graphite layer of about 200 g cm^{-2}, shows that a very big amount of electron-photon component can be generated occasionally in graphite in the core. This contribution of electron-photon component produced by N-particles is quite essential.

Miyake, S.: (to Dr. Zatsepin) About first point which you explained for Nikolsky's result, μ-meson is spread over large area. Then, even if his trigger is favorable to μ-meson, the tendency obtained by Dr. Sreekantan does not help to understand Nikolsky's result.

I understand the tendency as follows, if the number of N-component at the early stage is supposed to be large, μ-mesons will be produced in proportion to these N-particles, at the same time the effect of these N-particles still remaining in lower energy N-particles at later stage of development. If one takes the relation between μ-mesons and higher energy N-component, the tendency may be changed.

Zatsepin: The results of Nikolsky were not for very high energy N-particles, but for about 10^{10} ev. However, both Sreekantan and Nikolsky worked in the region within the distance of the order of 10 m from the core, where the energy spectrum is not very steep. Therefore, it may be possible that correlation of N-particles of 10^{10} ev with μ-mesons are the same as that of N-particles detected in neutron counter. On the other hand, if you pick up very high energy N-particles, say $10^{11}\sim10^{12}$ ev, I think that this correlation between N-particles and μ-mesons will disappear.

Dobrotin, N. A.: Sreekantan showed the comparison between N-particles associated and unassociated with EAS. The group of Grigorov showed that the proportion of N-particles associated and unassociated with EAS depends on the energy and hence on the dimension of the apparatus. Therefore, the slope of the spectrum would be different for different size of the apparatus. One has to be very careful to this effect.

JOURNAL OF THE PHYSICAL SOCIETY OF JAPAN Vol. 17, SUPPLEMENT A-III, 1962
INTERNATIONAL CONFERENCE ON COSMIC RAYS AND THE EARTH STORM Part III

III-4-19. Fluctuations and Correlations in the Fluctuations of Various Components of Extensive Air Showers

B. K. CHATTERJEE, G. T. MURTHY, S. NARANAN,
T. N. RANGA SWAMY, B. V. SREEKANTAN
and M. V. SRINIVASA RAO

Tata Institute of Fundamental Research, Bombay, India

§ 1. Introduction

An extensive air shower array comprising of the following units is in operation at mountain altitude of 800 g/cm² (Fig. 1) for the last nine months.

(a) 12 scintillators spread over an area of 80 m×80 m to measure the densities of charged particles at various distances from the core.

(b) 4 additional scintillators placed at the corners of a square of side 16 m, (in the centre of the array) coupled to a 45 channel nano-second chronotron timing equipment, to determine the angle of arrival of showers.

(c) 9 N-particle detectors each of area 0.4 m². clustered together at the centre of the array. Each detector is similar to the Simpson type neutron monitor and comprises of 4 BF_3 (enriched) counters surrounded by paraffin and lead. Cadmium sheets introduced in between the detectors prevent slow neutrons from one detector influencing the adjacent detector.

(d) 3 μ-meson detectors each of area of 0.6 m²: these consist of hodoscoped G-M counter trays. Two of the trays are under 5 ft. brick and 2″ of lead (≈ 20 radiation lengths) and the third under 750 g/cm² of iron (≈80 radiation lengths). In each tray there are 15 counters and these are connected to 5 hodoscope channels.

(e) One energy flow detector of area 0.36 m². located at the centre of the array —this consists of a scintillator placed under 2.5 cm lead.

(f) A total absorption spectrometer (120 cm×120 cm) described in detail in the following paper.

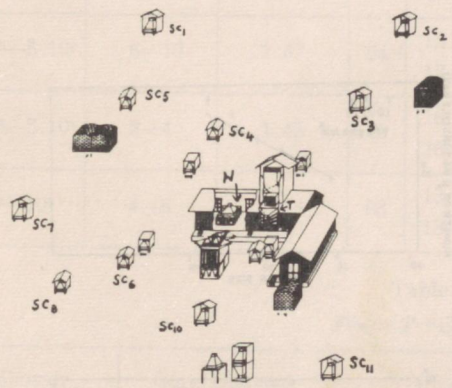

Fig. 1. Extensive Air Shower Array at Ootacamund (800 g/cm²)
$SC_1 \ldots SC_{12}$=Scintillation counters.
$CH_1 \ldots CH_4$=Fast scintillators for timing.
μ_1, μ_2=μ-meson detectors (1.8 m Bricks+5 cm Pb).
T=Total absorption spectrometer.
μ_3 is below the spectrometer (under 150 g/cm² Iron).
N=9 N-detectors at the centre of the array.

This array has been designed specifically to study fluctuations and correlations in the fluctuations of N-particles and μ-mesons. 20,000 showers have been recorded and about 5000 showers have been analysed on the electronic computer of the Tata Institute of Fundamental Research (TIFRAC). The main results are presented in the following sections.

2. Lateral Distribution of the Density of Charged Particles

For analysis on the computer the lateral distribution of the density of charged particles is assumed to have the form.

$$\Delta(r)=c(d)\cdot\frac{1}{r^{\alpha}}\cdot e^{-r/r_0}$$

where r is the distance from the core and α is a measure of the steepness of the lateral distribution near the core and r_0 is the

* This paper was combined with III-4-20, III-4-21 and presented by B. V. Sreekantan.

scattering length which has a value of 106 m for an altitude of 800 g/cm^2. Four values of α, *i.e.* 1.3, 1.5, 1.7, and 1.9 are tried for each shower and the computer prints out the best valve of α, the corresponding core position and shower size. The mean value of α increases with shower size as shown in Fig. 2. The increase was similar for vertical and inclined ($\theta > 40^0$) showers.

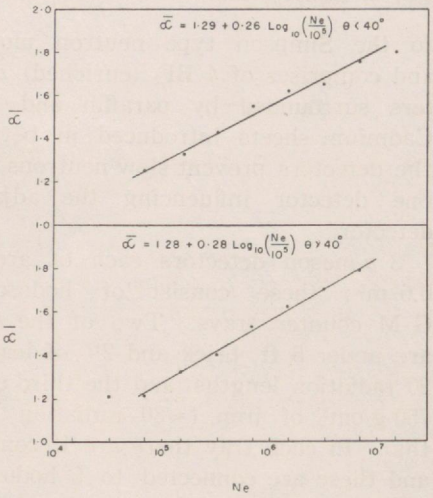

Fig. 2.

3. Variation of the Number of Nuclear Active Particles and μ-mesons with Shower Size

If the assumption is made that there are no large intrinsic fluctuations in the densities of N-particles in showers of the same N_e then the density $\Delta(N_e, r)$ is given by

$$\Delta(N_e, r) = \frac{1}{S\varepsilon m} \ln \frac{T}{T-Q}$$

where S is the area of N-detector, m is total number of detectors and ε is the efficiency of N-detectors, T is the total number of showers of size N_e with cores at distrance r from N-detectors. For our set-up $S=0.4$ m^2, $\varepsilon=0.25$, $m=9$. Using this procedure, the lateral distribution of the density of N-particles were determined up to a distance of 40 m from the core and by integrating the lateral distribution curves the number of nuclear active particles contained in a radius of 40 m around the core, were determined for various shower sizes. The results are shown in Fig. 3 (a) in which for

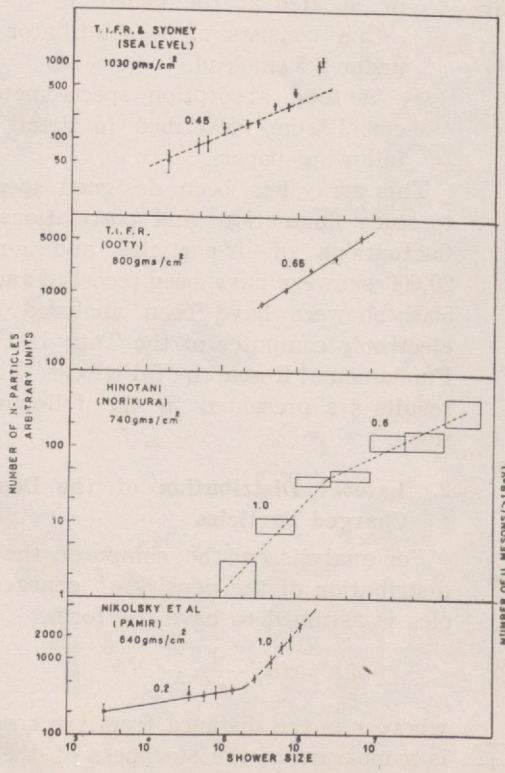

Fig. 3. (a)

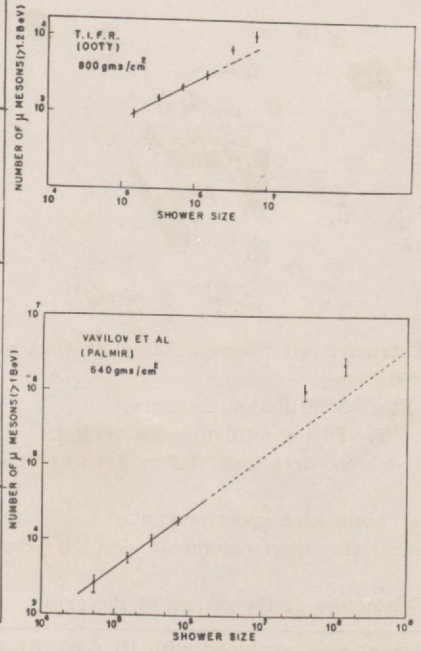

Fig. 3. (b)

comparison purposes similar results of other groups are also presented.

By a similar procedure and considering only the μ-meson detector under 750 g/cm^2 of iron, the variation of the number of μ-mesons within 40 m of the core, as a function of shower size was also determined. The results are shown in Fig. 3b, and compared with the results of others.

4. Fluctuations of N-particles and μ-mesons

In all experiments in which the total number of nuclear active particles or μ-mesons have been determined, the statistical procedure outlined in the previous section has been adopted, since it has not been possible to determine the lateral distribution of these components in individual showers. This method will lead to erroneous results if the number of nuclear active particles or μ-mesons fluctuate appreciably in showers of the same size. If the fluctuations are only poissonian, then the number $F(n)$ of showers in which 'n' out of 'm' N-detectors are activated is given by

$$F(n)=T\cdot P(n,\ \Delta) \qquad (2)$$

where $$P(n,\ \Delta)={}^mC_n[1-e^{-s\varepsilon\Delta}]^n\ e^{-s\varepsilon\Delta(m-n)} \qquad (3)$$

If the density of N-particles has a unique value for all showers of the same size, then

Table I. N-Particles

$F(n)=T\cdot {}^mC_n(1-e^{-s\varepsilon\Delta})^n e^{-s\varepsilon\Delta(m-n)}$

Shower Size (N_e)	Core Distance (in meters)	Δ (particles per m^2)	T	$F(n)$									
				0	1	2	3	4	5	6	7	8	9
5.10^6—10^7	10—15	2.11	40	6 6	8 12.6	9 12	6 6.5	4 2.3	5 0.54	0 0.08	0 0.008	2 5×10^{-4}	— —
10^6—2.10^6	4—6	2.85	13	1 1	1 2.97	2 4	1 3	1 1.5	1 0.5	3 0.1	3 0.015	— 1.3×10^{-3}	— —
10^6—2.10^6	6—10	1.12	129	47 47	29 50	22 24	14 6.6	5 1.2	4 0.14	3 0.01	4 6×10^{-4}	1 1.7×10^{-5}	— —
2.10^6—5.10^6	6—10	1.67	54	12 12	8 19.6	9 14.3	5 6	4 1.66	7 0.3	2 0.04	4 0.003	3 1.3×10^{-4}	— —
2.10^5—5.10^5	2—4	1.45	39	16 16	16 22.4	9 14	9 5.1	4 1.2	2 0.2	1 0.02	1 1.3×10^{-3}	1 5×10^{-5}	— —
5.10^5—10^6	4—6	1.75	63	13 13	10 22.4	11 17.2	11 7.7	5 2.2	6 0.42	4 0.05	3 4.4×10^{-3}	— —	— —

Table II. μ-Mesons

$F(n)=T\cdot {}^mC_n(1-e^{-s\varepsilon\Delta})^n e^{-s\varepsilon\Delta(m-n)}$

Shower Size (N_e)	Core Distance (in meters)	Δ (particles per m^2)	T	$F(n)$					
				0	1	2	3	4	5
5.10^6—10^7	15—25	1.53	64	26 26	19 25.7	12 10.1	5 2	1 0.197	1 0.007
2.10^6—5.10^6	15—25	1.2	87	43 43	21 32.5	11 9.85	7 1.5	3 0.13	2 0.034
10^6—2.10^6	15—25	0.85	125	76 76	26 39.8	13 8.3	7 0.87	2 0.046	1 0.0009
5.10^6—10^7	15—25	2.14	60	17 17	20 24.5	15 13.9	5 4	2 0.58	1 0.033

Table III. Correlation in fluctuations of N-particles and μ-mesons.

$$R=\frac{\text{Average No. of detectors activated for showers in which } \mu_1,\ \mu_2,\ \mu_3 \geq 1}{\text{Average No. of detectors activated for all showers}}$$

Shower size	Rn	$R\mu_1$	$R\mu_2$	$R\mu_3$
(2—5) 10^5	2.6±0.5	3.6±0.6	4.0±0.8	2.5±0.5
(5—10) 10^5	1.5±0.25	2.44±0.35	2.6±0.4	2.1±0.26
(1—2) 10^6	2.3±0.3	2.2±0.3	2.1±0.3	2.0±0.25
(2—5) 10^6	1.7±0.2	2.9±0.3	2.1±0.2	1.94±0.22
(1—2) 10^7	2.26±0.32	2.20±0.3	1.67±0.23	2.04±0.3
(2—5) 10^7	1.17±0.3	3.0±0.7	1.85±0.3	2.55±0.5
*(1—2) 10^7	4.2±0.9	2.5±0.6	2.7±0.7	2.9±0.7

* The group corresponds to showers in which $\mu_1,\ \mu_2,\ \mu_3 \geq 2$

Δ can be calculated from (1) and compared with the experimental distribution. This comparison has been made for N-particles in Table I and for μ-mesons by adopting an identical procedure, in Table II.

It is seen that the observed distribution deviates considerably from that calculated according to (1), (2), and (3). The deviation is more than what can be accounted for in terms of the finite width of size groups and core distances, chosen. It is therefore necessary to exercise a certain amount of caution in the interpretation of the curves presented in Fig. 3. To understand the full implications of those curves one should have all the data on fluctuations and the variation of fluctuations with size.

5. Correlations in the Fluctuations of N-Particles and μ-mesons

In order to see whether there exist correlations between the fluctuations of μ-mesons and N-particles the following procedure was adopted. The average number of μ-mesons that passed through any one of the μ-detectors was determined for the various shower sizes. From each particular size group those cases in which at least one μ-meson passed through each of the three μ-detectors (separated by more than 20 m) were picked up. For these cases the average number of μ-mesons passing through each of the detectors was calculated and compared with the average for all the showers of that size group. These ratios are given in Table III. For these cases in which the total number of μ-mesons had fluctuated, the average number of N-particle detectors that were activated was determined and compared with the average for all the showers. This ratio is also given in the Table III.

It is seen that the μ-mesons and N-particles fluctuate together and the order of fluctuation is of comparable magnitude.

Discussion

Discussion for Papers III-4-19, III-4-20 and III-4-21 is combined and given after the Paper III-4-21.